dMole: A Novel Transreceiver for Mobile Molecular Communication using Robust Differential Detection Techniques

Amit K. Shrivastava, Debanjan Das *Member, IEEE*, Rajarshi Mahapatra *Senior Member, IEEE* and Saraju P. Mohanty *Senior Member, IEEE*

***Abstract*—This paper proposes two differential detection techniques for signal detection in mobile molecular communication (MMC) for targeted drug delivery (TDD) application. In MMC, a nano-transmitter and a nano-receiver are considered to be in Brownian motion in an extracellular fluid medium. Transmitter uses calcium molecules to communicate with the receiver. Detection is performed using concentration difference based detector (CDD) at the receiver which calculates the maximum absolute concentration difference of the received signal within the same bit interval to detect the bit. This improves the bit error rate (BER) performance in MMC. The performance is further enhanced using manchester coded transmission with differential detection (MCD). In MCD, *Bit-1* is coded by the symbol [1 0] and *Bit-0* is coded by the symbol [0 1] and the difference between peaks of signals received in consecutive bit duration is taken to detect the bit. Simulation results prove that the MCD technique is 3 dB less sensitive to inter symbol interference (ISI) than the CDD technique. The detection threshold is selected using maximum a posteriori probability (MAP) rule. The performance of these detectors is compared with other existing detection techniques. Results reveal that BER performance of the CDD and MCD better by at least 3 dB and 6 dB, respectively. The proposed CDD and MCD techniques perform better in different bit-sequence length, various initial distance and different bit duration than other existing techniques.**

***Index Terms*—Mobile molecular communication, channel impulse response, detector design, inter symbol interference, targeted drug delivery.**

I. Introduction

In molecular communication (MC), natural and artificial nanomachines communicate among themselves by transmitting and receiving molecules [1]. Molecular communication is a new and interdisciplinary field. MC together with nano-technology independently has emerged as key players for the realization of futuristic smart healthcare system [2]. These group of nanomcahines form a nanonetwork. Communication in nanonetworks has opened several opportunities in advanced healthcare [3], [4], [5], [6], nano-robotics [7], environmental monitoring and wireless body area network [8].

In an MC system, nanomachines are the basic elements whose size can vary from nanometers to few micrometers [9]. These nanomachines can carry the drugs, which provide therapeutic actions in the human body during sickness. Drug carrying nanomachines used in TDD are shown in Fig. 1. These drugs must act on cells since the sickness is due to the disorder in cells. To increase the effectiveness of a therapeutic drug, it has to reach the target cell in the human body. In conventional drug delivery [10], such as oral ingestion and intravascular injection, the drug particles are distributed over the entire cardiovascular system from where they reach the diseased cells and perform therapeutic actions. In this case, only a small fraction of the inserted drug particles are delivered to the target cell. To deliver the drugs to the target site inside the body, the drug carrying nanomachines must reach near the diseased cells and perform drug delivery.

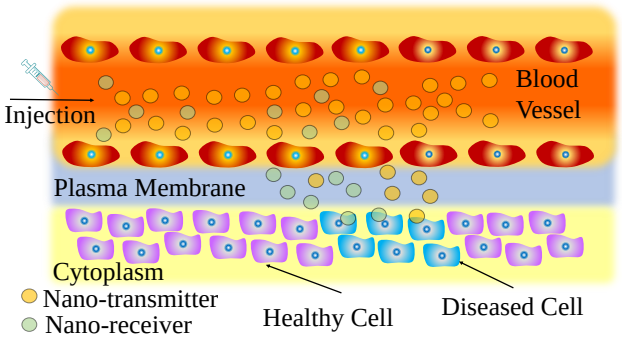

Fig. 1: Schematic representation of nanomachines targeting the disease cell in TDD applications.

While performing drug delivery, these nanomachines may be mobile and need to communicate with one another. Thus, investigation in mobile molecular communication (MMC) is the utmost necessary in TDD application [11], [12], [13]. In this work, we investigate various perspectives of mobile molecular communication. MMC requires robust transmission and detection mechanisms, which pose many challenges. The first challenge is the influence of the dynamic channel impulse response (CIR). During communication, transmitted molecules undergo random movement according to the Brownian motion. Based on Einsteins theory of diffusion, the CIR of the channel varies with time and distance between the nanomachines. The

Amit K. Shrivastava is with the Department of Electronics & Communication Engineering, International Institute of Information Technology Naya Raipur, Email: amits@iiitnr.edu.in.

Debanjan Das is with the Department of Electronics & Communication Engineering, International Institute of Information Technology Naya Raipur, Email: debanjan@iiitnr.edu.in.

Rajarshi Mahapatra is with the Department of Electronics & Communication Engineering, International Institute of Information Technology Naya Raipur, Email: rajarshi@iiitnr.edu.in.

Saraju P. Mohanty is with Department of Computer Science & Engineering, University of North Texas, Email: saraju.mohanty@unt.edu

concentration of molecules at the receiver first increases till a maximum value and then decreases slowly, forming a long tail [14].

The expected CIR in the case of static nano-transmitter and nano-receiver is only a function of time and is always the same. However, if either the nano-transmitter or the nano-receiver or both change their position continuously, then the CIR changes due to time-varying distance between them. This implies that, if the distance between the nano-transmitter and the nano-receiver decreases, the peak value of the CIR increases and the peak time decreases. Hence, if detection techniques for static MC are used, it poses challenges to accurate signal detection at the receiver. ISI is another challenge that makes detection difficult. The ISI occurs due to the long tail that occurs due to the molecules released during previous symbols. These previously released molecules may combine with receptor molecules at the receiver during the current bit duration. This causes incorrect signal detection. In MMC, the number of remaining molecules from a previously transmitted symbol varies because of the mobility of nanomachines. Hence existing techniques [14] used for detection and ISI mitigation in the case of static nano-transmitter and nano-receiver will not exhibit good performance for MMC. We propose two detection techniques based on the calculation of concentration difference for MMC which perform better than other existing detection techniques for MMC.

The rest of the paper is organized as follows: Section II describes the novel contributions of the paper. The related prior works has been surveyed in Section III. Section IV describes the proposed dynamic channel modeling based on Einsteins law of diffusion. Two different detection techniques proposed in the paper have been described in Section V. Section VI discusses the simulation results of the proposed techniques and compare their performance with other existing techniques. Finally, Section VII concludes the work with future scopes.

II. Novel Contributions of The Paper

In this paper, we propose differential detection techniques for mobile molecular communication (*dMole*), which has two transceiver techniques; concentration-difference based detector (CDD) and Manchester coded transmission with differential detection (MCD) techniques. Transmitter uses concentration shift keying (CSK), where some amount of molecules are sent to transmit a *B*it-1 and no molecules are transmitted to send *B*it-0. At the receiver, the signal is detected sample-wise and at each sample, the number of molecules is measured and the difference in concentration is calculated between two different samples. Fig. 2 shows the schematic diagram of the proposed MMC system. As shown in Fig. 2, transmitter sends signaling molecules to communicate with the receiver. These molecules arrive at the receiver which detects the information present in the molecules. The transmitter and receiver are mobile in the diffusive medium.

For detection, the concentration difference between the samples at time t_1 and t_2 in each bit interval is taken such that the absolute difference between the concentration at these samples is maximized. Then, the difference is compared with

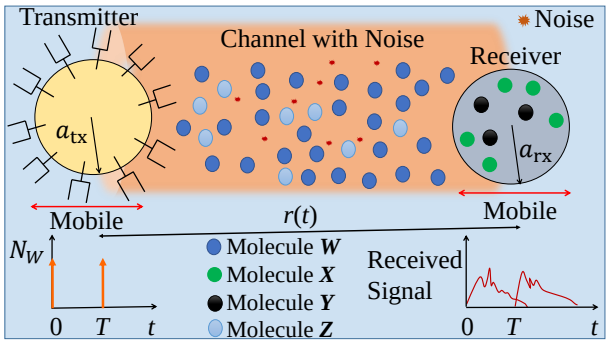

Fig. 2: Schematic diagram of the proposed mobile molecular communication system.

a threshold to make a decision in favor of *B*it-1 or *B*it-0. This gives a positive value of concentration difference when a *B*it-1 is received and a negative value of concentration difference when a *B*it-0 is received. The MCD technique, *B*it-0 is represented by symbol **[0 1]** and *B*it-1 is represented by the symbol **[1 0]**. The differential detector calculates the difference between peaks of received signal in consecutive bit duration. The difference is negative when *B*it-0 is received and the difference is positive when *B*it-1 is received. These techniques perform well in the diffusive medium where transmitter and receiver are mobile.

In summary, the **key contributions of the current paper** are the following:

- dMole, the differential detection techniques for robust performance in MMC environment for TDD application are proposed.
- A novel CDD technique has been proposed. The technique is relatively less sensitive to ISI, and perform better at a particular signal-to-noise ratio (SNR).
- The MCD, another novel transceiver technique has been proposed to improve ISI mitigation and better performance compared to CDD.
- The proposed detectors do not require an adaptive threshold for detection. They outperform the other existing detector for MMC.

III. Related Prior Works

Table I summaries the related prior works. The TDD is most promising of the techniques to deliver the drugs to the target site inside the body [10], [15], which ensures a smart localization of the desired amount of drugs at a reduced level of toxicity. TDD can be accomplished in two ways: First, the nanoparticles carrying drug molecules are inserted through the cardiovascular system, after which they reach the target site (MC only approach). Second, the nanomachines carrying drug molecules are implanted close to the target cells, bypassing the injection through the cardiovascular system (MC network approach). With this approach, the nanomachines can control the drug release rate by communicating through signaling molecules. This minimizes drug delivery to healthy parts of the body [16].

The model for particulate drug delivery system [17] considered the network of blood vessels as transmission line. This study was carried out for drug molecules as information carriers and no communication within the nanoparticles exist. For applications like TDD and in-body health monitoring, advanced techniques are required where communication between mobile nanomachines is also present [18], [19]. Mobile Nanomachines communicate among themselves to control the release of drug molecules [20], [21] inside the cells. A number of different works have been proposed for analysis of nano-communications [22], [23], coding schemes for error detection of multilevel cell memories [24], designing a mobile ad hoc molecular nanonetwork with molecular communication [25], fundamental understanding of nanonetworking [26], and Tcp like molecular communication [27].

Further, in MC, the detection techniques are an important reseearch topic. In recent years, several works related to detection for static transmitter and receiver in MC were considered [28]. Other techniques like asynchronous peak detectors with feedback were considered by Noel *et al*. [29]. Different variations of the weighted sum detector like an equal weight detector, matched filter detector were also studied [30]. However, more number of samples are required in an equal weight detector, while the matched filter detector is optimal in the presence of additive white gaussian noise only. Slope based detection (SBD) was studied in [31]. But in the presence of noise, it is likely to introduce errors because the slope values will change the sign rapidly in the presence of noise. A local convexity detection scheme has been proposed in [32]. For mobile transmitter and reeiver, simple technique for detection, single sample detector (SSD) was proposed in [33] but no noise and ISI were considered, a symbol detection scheme has been presented in [34]. Adaptive detection schemes like adaptive threshold detection based on peak time and adaptive threshold detection based on concentration were proposed in [35] where the threshold for detection can become incorrect if a long sequence of zeros is transmitted. Other adaptive detection schemes are presented in [36][37]. Cooperative abnormality detection is presented in [38]. Target detection in suspicious tissues has been presented in [39].

Further, the background noise present in the environment has been modeled as Poisson distributed [42]. The particle counting noise also exists which is due to the unwanted perturbation in the particle concentration measured at the receiver location around its expected value [43]. The particle counting noise is visible through two effects. The first effect is given by the quantization of the concentration measure by a discrete number of particles inside the receptor space. The second effect is given by fluctuations in the concentration measured due to single events of particles entering/leaving the receptor space [45]. The latter is more accentuated for high values of the particle concentration.

IV. Proposed Dynamic Channel Model in TDD Application

This section presents the channel model [33], [46] in the MMC system. Table II describes the notations used in this paper. Fig. 2 shows a schematic representation of the nano-transmitter and the nano-receiver. As shown in Fig. 2, a nano-transmitter of radius $a_{\rm tx}$ and a nano-receiver of radius $a_{\rm rx}$ with time-varying distance between them $r(t)$ are communicating with each other. W, X, Y, Z are different molecules. The spherical nano-transmitter of radius $a_{\rm tx}$ with diffusion coefficient $D_{\rm TX}$ and a spherical reactive nano-receiver of radius $a_{\rm rx}$ with diffusion coefficient $D_{\rm RX}$ separated by distance r_0 in an unbounded diffusion medium at 25^0C. The receiver is an artificial nanomachine that can release drug molecules based on the signaling molecules received from the transmitter nanomachine. The receiver surface contains R receptor molecules of type X and the shape of every receptor is assumed circular with radius r_s. The dynamic distance between nano-transmitter and nano-receiver is denoted by $r(t)$ where $r(t_0{=}0){=}r_0$. Further, it has been assumed that if, the nano-transmitter and the nano-receiver colloid with each other, they will be reflected back and their chemical properties will remain unaltered [33], [46]. Moreover, the nano-transmitter and the nano-receiver are not destroyed while communicating with each other.

Nano-transmitter uses type W molecules having diffusion coefficient D_W for signaling the nano-receiver. Each molecule of type W diffuses independently of other type W molecules. W molecule can be corrupted by the communication channel according to a first-order degradation reaction [33] as follows:

$$W \xrightarrow{C_d} Z, \tag{1}$$

where Z is the molecule unknown to the receiver and C_d is the degradation rate constant of the above reaction in s^{-1}. Further, when a W molecule reaches near the receiver, it reacts with a receptor molecule of type X following a second order reversible reaction [33]:

$$W + X \underset{C_b}{\overset{C_f}{\leftrightarrows}} Y, \tag{2}$$

where Y is an activated receptor molecule. C_f is the forward reaction rate constant for the receiver partially covered with receptors in $\mathrm{molecule}^{-1}\mathrm{m}^3\mathrm{s}^{-1}$ for the reaction described by (2). Also, an activated receptor molecule Y releases the information molecule W back into into the medium after a time governed by C_b [46]. C_b is the backward reaction rate constant in s^{-1} for the reaction described by (2). Further, it has been assumed that the molecules W are reflected after they unbind from receptor molecules X. Now, the Einstein's theory of diffusion [46] states that:

$$-J(r,t|r_0) = D_W \nabla P_W(r,t|r_0), \tag{3}$$

where $-J(r,t|r_0)$ is the incoming probability flux at the receiver's surface. ∇ is the gradient operator in spherical coordinates. $P_W(r,t|r_0)$ is the probability that a molecule W released from r_0 at time $t_0 = 0$ is at a position r at time t, and that this molecule can follow any of the two reactions given in Eqn. (1) and Eqn. (2). The CIR, $P_{WY}(t|r_0)$ is defined as the

TABLE I: Comparative perspective with related works

Work	**Year**	**Key contributions**	**Channel**	**Application**
Requicha, *et al.* [9]	2003	Design, fabrication, and programming of robots of size few micrometers	-	Environmental monitoring and health care
Cavalacanti, *et al.* [40]	2006	Guiding nanorobots to identify malignant tissues using chemical gradient	Blood vessel	Targeting the cancer tumour
Akyilidz, *et al.* [26]	2008	Communication at different ranges	-	Biomedical applications, Immune system support
Shah, *et al.* [28]	2012	MosK modulation, Optimum receiver using MAP criterion, BER $\approx 10^{-6}$	Static, Blood at 310K	Drug delivery, disease detection
Chahibi, *et al.* [41]	2013	Proposes drug propagation network model to find the drug delivery rate at the targeted site	Mobile, Model cardiovascular system as transmission line network	Drug delivery
Gelenbe, *et al.* [22]	2015	Magnetic spin based communication (minimum error probability achieved 0.1)	-	-
Femminella, *et al.* [16]	2015	Reception model as pure loss queuing systems (M/M/1/1 queue model for each receptor), Blocking probability (0.05 at $100\mathrm{mol/s}$)	Static, Extracellular matrix	Drug delivery
Tepekule, *et al.* [14]	2015	MTSK modulation, Decision feedback filter (DFF) at receiver to find optimal threshold, BER $\approx 10^{-4}-10^{-6}$	Static, liquid with diffusion coefficient $74\mu\mathrm{m}^2/\mathrm{s}$	Drug delivery
Farsad, *et al.* [18]	2016	Presents different type of molecular communication. Various modulation, coding techniques, simulation tools summarized.	-	Artificial immune system, robotic communication in harsh environments like sewer system
Okonkwo, *et al.* [10]	2017	Discusses challenges of channel modeling inside human body, design of nanosystems	-	Drug delivery, health monitoring
Nakano, *et al.* [11]	2017	Finds likelihood of tumour site detection using chemical attractants	Extracellular matrix, cells	Drug delivery
Ahmadzadeh, *et al.* [33]	2017	Channel modeling for mobile molecular communication, SSD technique, BER $\approx 2\times10^{-4}$, Data rate $333\mathrm{bps}$	Mobile, Water at 25^0 C	Drug delivery
Yan, *et al.* [31]	2017	Derivative based detection for molecular communication, SBD technique, BER $\approx 10^{-5}$, Data rate $370\mathrm{bps}$	Static	Drug delivery
Farsad, *et al.* [42]	2018	Deep learning based detection, BER $\approx 10^{-5}$, Data rate $2\mathrm{bps}$.	Static for molecular channel, dynamic for optical channel	Health monitoring
Alshammri, *et al.* [43]	2018	Adaptive fuzzy threshold based detection, BER $\approx 10^{-5}$	Static	Drug delivery, lab on a chip
Chang, *et al.* [44]	2018	Adaptive threshold based detection, BER $\approx 10^{-4}$, Data rate $\approx 10\mathrm{bps}$	Dynamic	Drug delivery
Tavella, *et al.* [2]	2019	Encodes information through bacterial nanonetworks	-	Drug delivery
Okonkwo, *et al.* [3]	2019	Discusses molecular communication aspects for treatment of chronic diseases	Human organ	Drug delivery
Kassab, *et al.* [4]	2019	Proposes blockchain techniques for healthcare	-	Healthcare
Jiang, *et al.* [8]	2019	Proposes fuzzy commitment based key agreement based protocol for wireless body area network	-	Securing health data
Guney, *et al.* [25]	2019	Evaluate the performance of nanonetwork based on average message delivery delay and incurred traffic rate	Mobile, Neurospike channel	Drug delivery
Current paper	2020	Proposes CDD and MCD technique for signal detection, BER $\approx 10^{-4}$, Data rate $10\mathrm{bps}$	Mobile, Extracellular fluid	Drug delivery

TABLE II: Symbol and Notation Definitions.

Symbol/ Notation	Parameters
N_W	Number of molecules released by the transmitter
D_W	Diffusion coefficient of a W molecule
D_{TX}	Diffusion coefficient of the transmitter
D_{RX}	Diffusion coefficient of the receiver
a_{tx}	Radius of the transmitter
a_{rx}	Radius of the receiver
C_f	Forward reaction rate constant
C_b	Backward reaction rate constant
C_d	Degradation rate constant
r_0	Initial distance between nanomachines
L	Number of bits transmitted
t_s	Sampling time
T	Bit duration
r_s	Radius of receptor molecules X on the receiver
R	Number of receptor molecules X on the receiver
θ	Temperature of the medium
W, X, Y, Z	Types of molecules
$P_{WY}(t\|r_0)$	Conditional probability that W molecule transmitted from r_0 at t_0=0 activates a receptor molecule X at a time t
ζ	Fraction of receiver's area covered by receptor molecules
PMF	Probability Mass Function
CDD	Concentration difference based detector
MCD	Manchester coded transmission with differential detection
d_{CDD}	Concentration difference for CDD
d_{MCD}	Concentration difference for MCD

conditional probability that a W molecule transmitted from r_0 at t_0=0 activates a receptor molecule X at a time t [33]:

$$P_{WY}(t|r_0) = \frac{C_f e^{-C_d t}}{4\pi r_0 a_{\mathrm{rx}}\sqrt{D_W}} \begin{bmatrix} \frac{aU(f(t),a\sqrt{t})}{(c-a)(a-b)} \\ +\frac{bU(f(t),b\sqrt{t})}{(b-c)(a-b)} \\ +\frac{cU(f(t),c\sqrt{t})}{(c-a)(b-c)} \end{bmatrix}, \quad (4)$$

where $U(\alpha,\beta) = exp(2\alpha\beta+\beta^2)erfc(\alpha+\beta)$. $erfc()$ is the complementary error function, $f(t) = (r_0 - a_{\mathrm{rx}})/\sqrt{4D_W t}$. CIR can be found by integrating (3) over the surface area of the receiver and time t. The CIR defined in (4) takes into account, the diffusion of the transmitted molecules W through the medium, as well as, degradation of the W molecules in the medium and reaction of W molecules with receptor molecules X. Hence, it is a function of D_W, C_d, C_f and C_b.

The values of C_f, C_b and C_d decide the number of W molecules bound by the receiver [46]. Increasing C_f and decreasing C_b will enhance the number of received molecules. Decreasing C_f and increasing C_b will reduce the number of received molecules. Also increasing C_d will decrease the number of received molecules because more molecules of type W will be degraded in the medium. Hence, the probability that a W molecule reaches the receiver and binds to the receptor on the receivers surface depends on C_f, C_b and C_d. The parameters a, b and c are the solutions of the following expressions [33]:

$$a+b+c = \left[1+\frac{C_f^*}{4\pi D_W a_{\mathrm{rx}}}\right]\frac{\sqrt{D_W}}{a_{\mathrm{rx}}}, \quad (5)$$

$$ab+bc+ca = C_b - C_d, \quad (6)$$

$$abc = C_b\frac{\sqrt{D_W}}{a_{\mathrm{rx}}} - C_d\left[1+\frac{C_f^*}{4\pi D_W a_{\mathrm{rx}}}\right]\frac{\sqrt{D_W}}{a_{\mathrm{rx}}}, \quad (7)$$

where,

$$C_f^* = \frac{4\pi D_W C_f \psi}{C_f a_{\mathrm{rx}}(1-\psi)+4\pi D_W}, \quad (8)$$

$$\psi = \frac{Rr_s^2(C_f a_{\mathrm{rx}}+4\pi D_W)}{a_{\mathrm{rx}}^2(1-\zeta)(\pi r_s C_f+16\pi D_W)+Rr_s^2(C_f a_{\mathrm{rx}}+4\pi D_W)}, \quad (9)$$

and

$$\zeta = R\left(\frac{\pi r_s^2}{4\pi a_{\mathrm{rx}}^2}\right). \quad (10)$$

A receiver whose surface is partially covered with receptors with forwarding reaction rate constant C_f is approximately similar to the receiver whose surface is fully covered with receptors and altered forward reaction rate constant C_f^* [46].

This channel model will be extended for the proposed MMC system, where the dynamic nature of the channel is considered. This dynamic channel model explains the behavior of a mobile channel, where the nano-transmitter and the nano-receiver are changing their position according to Brownian motion. Co-ordinates of transmitter nanomachine are assumed to be $(x_{\mathrm{tx}}(t), y_{\mathrm{tx}}(t), z_{\mathrm{tx}}(t))$ and coordinates of receiver nanomachine are assumed to be $(x_{\mathrm{rx}}(t), y_{\mathrm{rx}}(t), z_{\mathrm{rx}}(t))$. Since the motion of nanomachines is assumed to be Brownian, their co-ordinates change according to the following expressions:

$$x_{\mathrm{tx}}(t+t_s) = x_{\mathrm{tx}}(t) + \eta(0, 2D_{\mathrm{TX}}t_s), \quad (11)$$

$$y_{\mathrm{tx}}(t+t_s) = y_{\mathrm{tx}}(t) + \eta(0, 2D_{\mathrm{TX}}t_s), \quad (12)$$

$$z_{\mathrm{tx}}(t+t_s) = z_{\mathrm{tx}}(t) + \eta(0, 2D_{\mathrm{TX}}t_s), \quad (13)$$

$$x_{\mathrm{rx}}(t+t_s) = x_{\mathrm{rx}}(t) + \eta(0, 2D_{\mathrm{RX}}t_s), \quad (14)$$

$$y_{\mathrm{rx}}(t+t_s) = y_{\mathrm{rx}}(t) + \eta(0, 2D_{\mathrm{RX}}t_s), \quad (15)$$

$$z_{\mathrm{rx}}(t+t_s) = z_{\mathrm{rx}}(t) + \eta(0, 2D_{\mathrm{RX}}t_s). \quad (16)$$

In the above expressions, $\eta(0,\sigma^2)$ is a normally distributed random variable with mean zero and variance σ^2. The instantaneous distance between nanomachines can be calculated as:

$$r(t) = \sqrt{\begin{matrix}[x_{\mathrm{rx}}(t)-x_{\mathrm{tx}}(t)]^2+[y_{\mathrm{rx}}(t)-y_{\mathrm{tx}}(t)]^2+ \\ [z_{\mathrm{rx}}(t)-z_{\mathrm{tx}}(t)]^2\end{matrix}}. \quad (17)$$

In the present system model under consideration, a molecule W diffuses with the diffusion coefficient D_W and a receptor molecule X mounted on the receiver diffuses with the diffusion coefficient D_{RX}. Therefore, the relative diffusion coefficient D_1 of a molecule W with respect to a molecule X is given by the following expression [33]:

$$D_1 = D_W + D_{\mathrm{RX}}. \quad (18)$$

Now, if the transmitter and the receiver are mobile, the CIR is given by Eqn. (4) if we substitute D_1 in Eqn. (18) in place

of D_W in Eqn. (4) and r_0 is replaced by $r(t)$. The expected received signal is given by the following:

$$\bar{N}_{Y\text{total}}(i,k) = \sum_{j=0}^{I} N_{i-j} P_{WY}(h(k) + jT | r_{i-j}) + m_n, \quad (19)$$

where $N_{Y\text{total}}(i,k)$ is the total signal received at kth sample during ith bit duration, $N_{i-j} = N_W$ if $b_{i-j} = 1$ and $N_{i-j} = 0$ if $b_{i-j} = 0$ or $i - j < 0$. $h(k) = kt_s$ are the sampling times. The constant I is the number of previous symbols that cause ISI in the current symbol interval. Further, $r_0, r_1, r_2 ... r_{L-1}$ are the distances between nanomachines at the begining of symbol intervals $0, 1, 2, ..., (L-1)$ respectively. The external noise is modeled as a poisson random variable with mean value m_n [47].

The proposed dynamic channel model will apply in the TDD application. Fig. 3 represents the scenario in which the present model can be useful. As shown in the figure, the transmitter nanomachine (controller nanomachine) first sense the number of drug molecules required to be delivered inside the ECF (Extracellular fluid), surrounding a cell (ECF is the fluid which surrounds the cell), then it can send appropriate commands to the receiver nanomachine so that receiver nanomachine (carrying drug molecules) can deliver the drug in proper dose [16]. As an example, when a transmitter nanomachine sends some commands to receiver nanomachine by using signaling molecules, the commands can be sent in the form of bits:

- [0 0] - Start releasing drug molecules.
- [0 1] - Increase the quantity of drug molecules.
- [1 0] - Decrease the quantity of drug molecules.
- [1 1] - Stop delivering drug molecules.

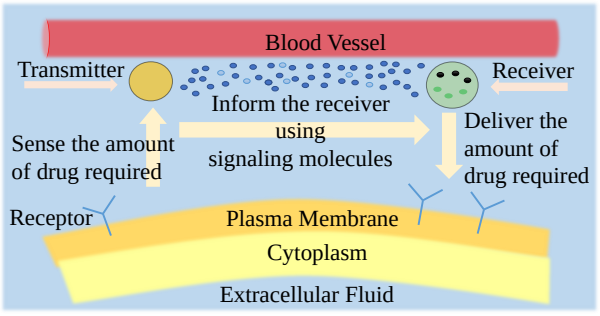

Fig. 3: Transmitter nanomachine (controller nanomachine) first sense the amount of drug molecules required to be delivered inside the ECF, then it can send appropriate commands to the receiver nanomachine so that receiver nanomachine (carrying drug molecules) can deliver the drug in proper dose.

The receiver is an artificial nanomachine that can release drug molecules based on the signaling molecules received from the transmitter nanomachine. Such control will be required to deliver an appropriate dose of drug molecules. Noise and ISI often occur during this communication. Problems due to noise and ISI can be understood with the following example. The receiver nanomachine will receive commands in the form a bit sequence. If due to ISI, command **[0 1]** is interpreted as **[1 1]**, then instead of increasing the number of therapeutic molecules, the delivery of therapeutic molecules will be stopped and the task of TDD will not be accomplished properly.

V. dMOLE: THE PROPOSED TRANSMISSION AND DETECTION TECHNIQUES

In this section, we will discuss the transmission and detection techniques proposed in this paper which are suitable for MMC. Transmitter uses CSK as the modulation technique. An impulse of N_W molecules is sent by the transmitter to transmit *Bit-1* and no molecules are sent for *Bit-0*. Noise is modeled as Poisson distributed with mean value of m_n [47]. The receiver detects the signaling molecules using the CDD technique.

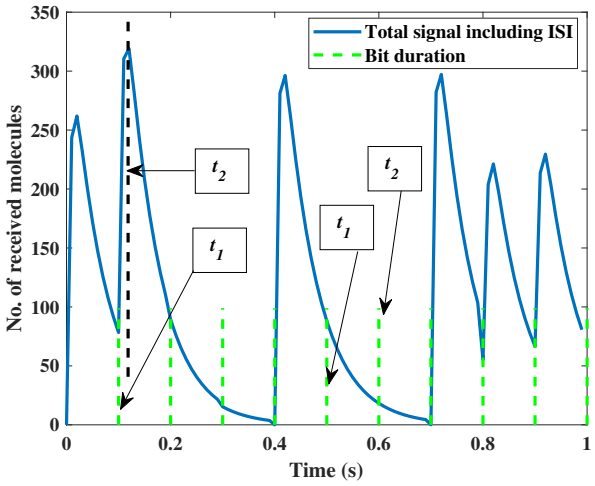

Fig. 4: The received signal in case of CDD for **10** bit durations without noise when the transmitted sequence is **[1 1 0 0 1 0 0 1 1 1]**.

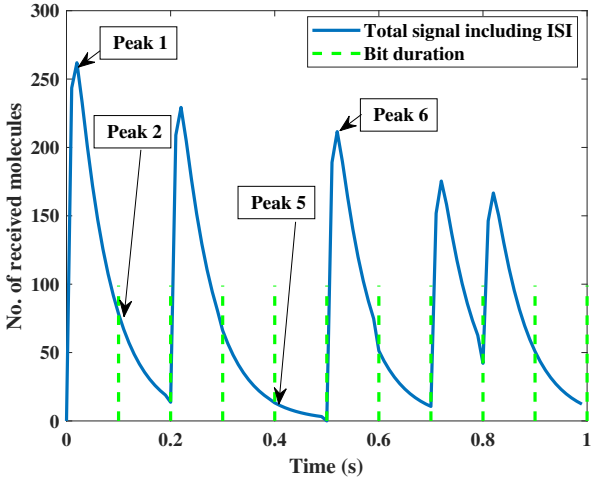

Fig. 5: The received signal in case of MCD for **10** bit durations without noise when the transmitted sequence is **[1 1 0 0 1]**.

In order to enhance robustness to ISI, the MCD technique is used. Assuming that the number of bits L sent by the transmitter as $b = [b_0, b_1, b_2, ..., b_{L-1}]$, where b_j is the transmitted

bit in the jth interval. The bit interval is denoted by T. In this paper, two different strategies for detection are presented as discussed in the subsequent subsections.

A. Transmission with CSK and Detection with CDD

In this case, N_W molecules (say, 10000) of type W are transmitted to send *Bit-1* and no molecules are transmitted to send *Bit-0*. The received signal corresponding to this transmission strategy is shown in Fig. 4. CDD is used to detect whether the transmitted bit was a *Bit-0* or a *Bit-1*. For detection, the difference between the concentration at two different time instants t_2 and t_1 within each symbol interval is calculated such that the absolute difference $|N_{Y\text{total}}(i,t_2) - N_{Y\text{total}}(i,t_1)|$ is maximized:

$$\underset{t_2}{\operatorname{argmax}} \, |N_{Y\text{total}}(i,t_2) - N_{Y\text{total}}(i,t_1)|. \tag{20}$$

In the above expression, t_1 is constant and t_2 is a variable. t_1 is the starting time of a bit interval and t_2 is selected such that absolute concentration difference between time t_2 and t_1 is maximized. So, in case of bit-1, t_2 is the time where peak concentration occurs (which changes with distance in MMC) and in case of bit-0, t_2 is at time at which minimum concentration value occurs (t_2 may also differ slightly in each bit interval due to noise but it will be near to the end of bit interval). Then the decision metric for detection in (21) is the concentration difference between these two times (not absolute concentration difference). Detection is performed using following rule:

$$\hat{b}_i = \begin{cases} 1 & \text{if } [N_{Y\text{total}}(i,t_2) - N_{Y\text{total}}(i,t_1)] > 0, \\ 0 & \text{otherwise.} \end{cases} \tag{21}$$

$\hat{b}_i$ denotes the estimated bit in ith bit interval. Detection threshold can be set to zero because this concentration difference is positive if *Bit-1* is received and negative if *Bit-0* is received. Threshold can also be determined as the point of intersection of conditional probability plots $P(d_{\text{CDD}}|b_j = 1)$ and $P(d_{\text{CDD}}|b_j = 0)$ in Fig. 6(a). d_{CDD} is the difference given by (21) and $P(d_{\text{CDD}}|b_j)$ is the conditional probability of obtaining a concentration difference d_{CDD} given that bit b_j is transmitted. Concentration difference in the case of *Bit-0* is negative due to ISI. Thus ISI is desirable in this detection technique. Also, synchronization [48] between nanomachines is required for detection.

B. Manchester Coded Transmission with Differential Detection (MCD)

In the present technique, *Bit-1* is coded as symbol **[1 0]** and *Bit-0* is coded as symbol **[0 1]**. Then CSK is used as the transmission technique. The received signal corresponding to this transmission strategy is shown in Fig. 5. The differential detector calculates the difference between peaks of consecutive bits in a symbol as shown in the Fig. 5. This difference is positive when symbol **[1 0]** is received (Peak 1 - Peak 2 in Fig. 5) and the difference is negative when symbol **[0 1]** is received (Peak 5 - Peak 6 in Fig. 5). The differential detector calculates the difference between peaks of consecutive bits in a symbol shown in braces $(0,1),(2,3),(4,5)...(2L-2,2L-1)$. If we denote maximum value of $N_{Y\text{total}}(i,k)$ by $\max(i,k)$ then detection rule of this detector is given by:

$$\hat{b}_i = \begin{cases} 1 & \text{if } [\max(2i,k) - \max(2i+1,k)] > 0, \\ 0 & \text{otherwise.} \end{cases} \tag{22}$$

Detection threshold can be determined as the point of intersection of conditional probability plots $P(d_{\text{MCD}}|b_j = 1)$ and $P(d_{\text{MCD}}|b_j = 0)$ in Fig. 6(b). d_{MCD} is the difference given by (22). The performance of these techniques is compared with two other existing detection techniques slope based detector (SBD) and the single sample detector (SSD) as described in Eqn. (23) and Eqn. (24), respectively.

Detection rule of the SBD [31] is given by:

$$\hat{b}_i = \begin{cases} 1 & \text{if } \max(\frac{N_{Y\text{total}}(i,k+1) - N_{Y\text{total}}(i,k)}{t_s}) > \lambda_1, \\ 0 & \text{otherwise.} \end{cases} \tag{23}$$

λ_1 is the detection threshold used by SBD. The detection rule of the SSD [33] is given by the following expression:

$$\hat{b}_i = \begin{cases} 1 & \text{if } N_{Y\text{total}}(i,4) > \lambda_2, \\ 0 & \text{otherwise.} \end{cases} \tag{24}$$

λ_2 is the detection threshold used by SSD.

TABLE III: Simulation Parameters.

Param.	Value	Param.	Value
N_W	10000	L	100
D_W	$1.01 \times 10^{-9}\text{m}^2/\text{s}$	t_s	0.01s
D_{RX}	$2.31 \times 10^{-12}\text{m}^2/\text{s}$	T	0.1s
r_0	$5\mu\text{m} - 20\mu\text{m}$	r_s	0.114nm
a_{rx}	$0.05\mu\text{m}$	R	2000
C_f	$12.5 \times 10^{-15} \frac{\text{m}^3}{\text{molecule}\cdot\text{s}}$	C_d	110s^{-1}
C_b	1000s^{-1}	D_{TX}	$4.74 \times 10^{-12}\text{m}^2/\text{s}$
a_{tx}	$0.024357\mu\text{m}$	θ	25^0C

VI. Experimental Results

In this section, we will present the performance of the proposed techniques and compare them with existing techniques. In the present study, we have considered ECF at 25^0C as the diffusion medium and type W molecules are selected as calcium molecules. The typical values of the different parameters used in the simulation are shown in Table III and Monte-Carlo simulation has been used to obtain the results. The average value of BER has been obtained after 100 iterations, where each iteration has a different value of $r(t)$.

Also, different sequences of 100 bits are used in each iteration. The signal to noise ratio (SNR) is defined as [49]:

$$SNR = 10\log_{10}\left[\frac{E(\sum_{i=0}^{L-1}(\max(N_{Y\text{total}}(i,k)))^2)}{Lm_n}\right]. \tag{25}$$

The calculation of SNR is shown in the APPENDIX A. Since the external noise is modeled as a Poisson random variable [47], its mean and variance are equal to m_n. In the denominator of (25), m_n denotes the variance.

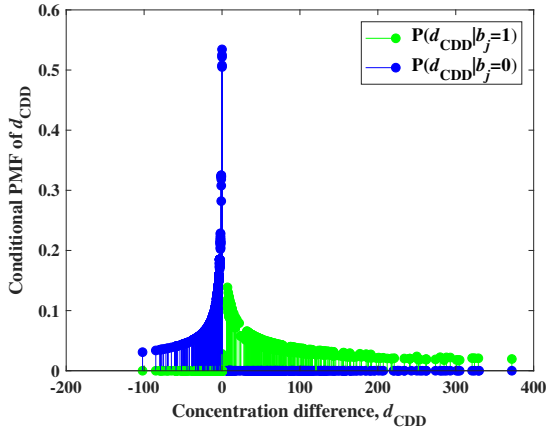

(a) Conditional PMF of d_{CDD}

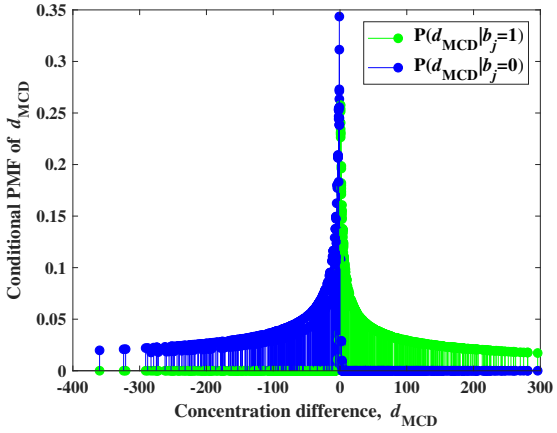

(b) Conditional PMF of d_{MCD}

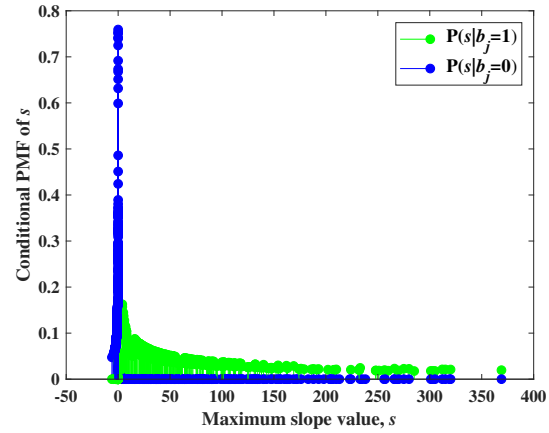

(c) Conditional PMF of slope s

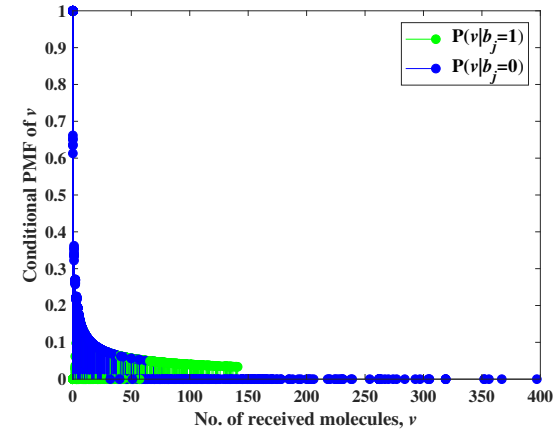

(d) Conditional PMF of number of received molecules v

Fig. 6: Conditional PMF for different parameters of proposed techniques.

A. Determining the threshold using maximum a posteriori probability (MAP) criterion

This section describes the probability mass functions obtained for all the detectors and thresholds are found using the MAP criterion. If Z is the received signal, $P(1)$ is the apriori probability that *Bit-1* is transmitted and $P(0)$ is the apriori probability that *Bit-0* is transmitted and $P(1|Z)$, $P(Z|1)$ are the conditional probabilities then MAP rule states that:

$$\hat{b}_i = \begin{cases} 1 & \text{if } P(1|Z) > P(0|Z), \\ 0 & \text{otherwise.} \end{cases} \tag{26}$$

or

$$\hat{b}_i = \begin{cases} 1 & \text{if } P(Z|1)P(1) > P(Z|0)P(0), \\ 0 & \text{otherwise.} \end{cases} \tag{27}$$

If $P(0)$=$P(1)$ then MAP rule reduces to the following:

$$\hat{b}_i = \begin{cases} 1 & \text{if } P(Z|1) > P(Z|0), \\ 0 & \text{otherwise.} \end{cases} \tag{28}$$

Probability mass function (PMF) of CDD, MCD, and SBD follows a skellam distribution [50] which is the distribution of the difference between two Poisson distributed random variables. Since the received signal follows a Poisson distribution [33], the difference between the received signal at two different sampling times, follows a skellam distribution given by:

$$P(D=d) = e^{-(\mu_1+\mu_2)} \left(\frac{\mu_1}{\mu_2}\right)^{d/2} I_d(2\sqrt{\mu_1\mu_2}) \tag{29}$$

where $P(D=d)$ is the probability that difference D is equal to $d = N_1 - N_2$. N_1 and N_2 are poisson distributed random variables with mean μ_1 and μ_2, respectively. I_d is the modified Bessel function of first kind. Fig. 6(a)(b)(c) are plotted using (29). We denote d_{CDD} as the difference given by (21), d_{MCD} as the difference given by (22) and $s = \max(N_{Y\mathrm{total}}(i, k+1) - N_{Y\mathrm{total}}(i,k)$ is the numerator of (23) because multiplying t_s in (23) to R.H.S. makes no difference in (23). Now, from Fig. 6(a) it can be observed that:

$$\begin{cases} P(d_{\mathrm{CDD}}|b_j=1) > P(d_{\mathrm{CDD}}|b_j=0) & \text{if } d_{\mathrm{CDD}} > 0 \\ P(d_{\mathrm{CDD}}|b_j=1) < P(d_{\mathrm{CDD}}|b_j=0) & \text{if } d_{\mathrm{CDD}} < 0. \end{cases} \tag{30}$$

Hence, the threshold for CDD can be selected as **0**.

Also from Fig. 6(b), it can be observed that:

$$\begin{cases} P(d_{\mathrm{MCD}}|b_j=1) > P(d_{\mathrm{MCD}}|b_j=0) & \text{if } d_{\mathrm{MCD}} > 0 \\ P(d_{\mathrm{MCD}}|b_j=1) < P(d_{\mathrm{MCD}}|b_j=0) & \text{if } d_{\mathrm{MCD}} < 0. \end{cases} \tag{31}$$

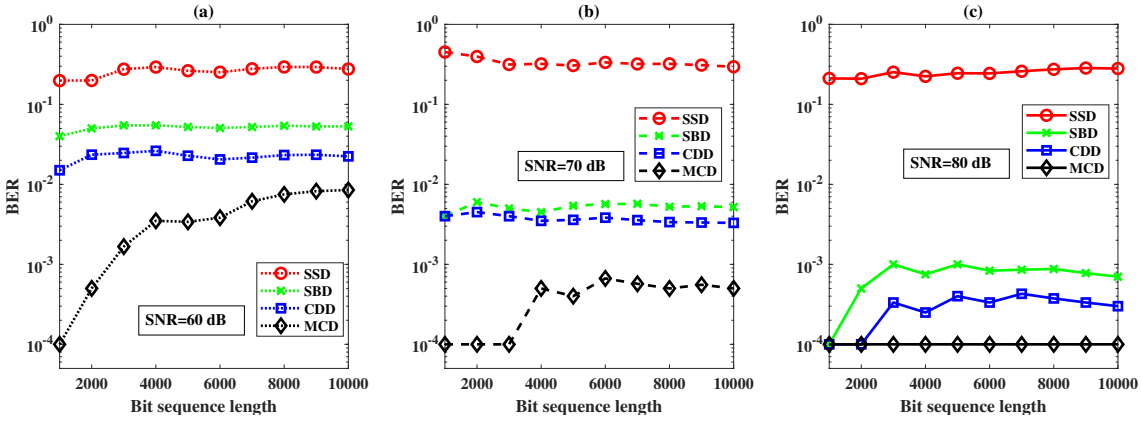

Fig. 7: Variation of BER with bit-sequence length for different detection techniques at different SNR (a) 60 dB, (b) 70 dB and (c) 80 dB.

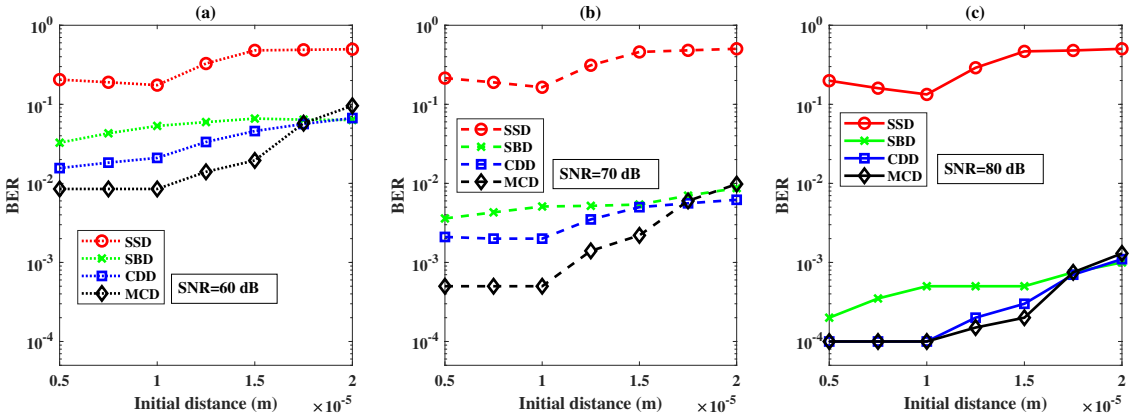

Fig. 8: BER performance with initial distance between nanomachines for different detection techniques at different SNR (a) 60 dB, (b) 70 dB and (c) 80 dB.

Hence, the threshold for MCD can also be selected as $\mathbf{0}$. Similarly, threshold for slope based detector can also be selected as $\mathbf{0}$. CDD and MCD perform better than SBD because, for SBD, most of the values of s (given that *Bit-0* was transmitted) are negative values which are very close to zero (Fig. 6(c)). Slight noise level can shift the value of s to a positive value where $P(s|b_j = 1) \approx P(s|b_j = 0)$.

PMF of SSD follows a Poisson distribution given by the following expression:

$$P(V = v) = \frac{\bar{N}_{Y\text{total}}(i,k)^v e^{-\bar{N}_{Y\text{total}}(i,k)}}{v!}, \qquad (32)$$

where V is the random variable denoting the number of molecules received. From Fig. 6(d) it can be observed that:

$$\begin{cases} P(v|b_j = 1) < P(v|b_j = 0) & \text{if } v < 5 \\ P(v|b_j = 1) \approx P(v|b_j = 0) & \text{if } 5 < v < 100 \\ P(v|b_j = 1) > P(v|b_j = 0) & \text{if } v > 100. \end{cases} \qquad (33)$$

The second condition in Eqn. (33) is due to the ISI. Hence, it is difficult to find a threshold for SSD in the case of MMC system. MAP criteria are satisfied only for first and third conditions in Eqn. (33), therefore BER is high in case of SSD as evident from the simulation (Fig. 7 and Fig. 8).

B. Impact of bit-sequence length on BER

The impact of increasing bit sequence length on BER for the different detectors is shown in Fig. 7. At 60 dB SNR, BER values become large for all detectors because, during transmission of more amount of bits, the distance between the nanomachines may increase and fewer molecules might reach the receiver. This effect can be reduced by increasing the SNR to 80 dB. A high value of SNR is required in MMC relative to static MC [49]. This is because the distance between nanomachines may increase leading to insufficient signal power if less value of SNR is used. At different SNR values, CDD gives a better performance than SBD and SSD. Also, MCD outperforms other detectors.

C. Impact of the initial distance between nanomachines on BER

Distance between nanomachines also affects the BER value. The impact of the initial distance on BER for different detectors is shown in Fig. 8. It has been observed that beyond 20μm, the signal received is almost zero. As the distance increases, the number of molecules that reach the receiver decreases thereby increasing the BER for all the detectors. In this case also, MCD gives the lowest BER values.

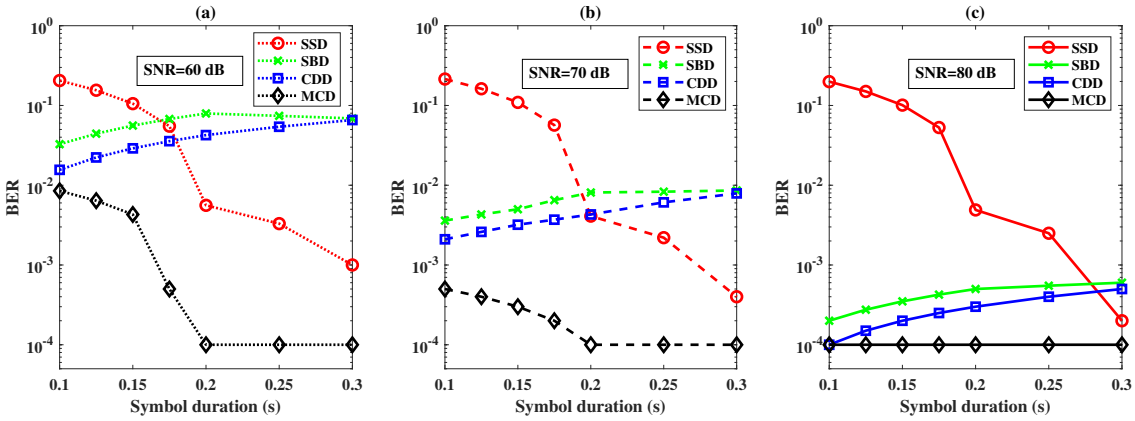

Fig. 9: BER versus bit duration for different detection techniques at different SNR (a) 60 dB, (b) 70 dB and (c) 80 dB.

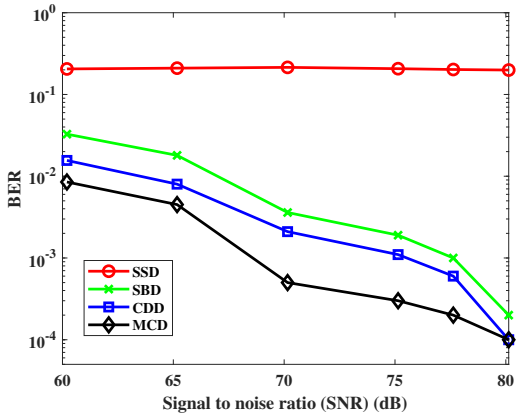

Fig. 10: BER versus SNR plots for different detection techniques).

D. Variation of BER with bit-duration

Fig. 9 shows the variation of BER with bit duration for different detectors for different SNR values. It can be observed that SSD performs better at larger bit durations because ISI reduces with an increase in bit duration. SBD and CDD perform better for small values of bit duration because they utilize ISI for detection of *Bit-0* and their performance degrades with an increase in bit duration because the ISI reduces with an increase in bit duration.

E. Variation of BER with SNR

Fig. 10 shows the BER performance of all the detectors with SNR. The SNR has been defined in (25). As the SNR increases, BER for all detectors except SSD shows a decreasing trend. SSD does not exhibit a significant decrease in the BER. This is because an increase in SNR increases the amount of ISI also. For SBD, CDD, and MCD the BER decreases with SNR indicating that noise has less impact on BER for these detectors as the SNR increases. Further CDD and MCD perform better than SBD because SBD is more sensitive to noise which can be understood from (23). Since, $N_{Y\text{total}}(i,k{+}1)$ and $N_{Y\text{total}}(i,k)$ are adjacent samples, their values can fluctuate rapidly in presence of noise and their difference can be negative where it is expected to be positive. CDD is less sensitive to noise because $N_{Y\text{total}}(i,t_2)$ and $N_{Y\text{total}}(i,t_1)$ are not adjacent samples. The concentration difference in (21) gives the largest concentration difference which is positive for *Bit-1* and negative for *Bit-0* as shown in Fig. 4. For, MCD the concentration difference given by (22) is positive for *Bit-1* as it is coded by symbol **[1 0]** and concentration difference given by (22) is negative for *Bit-0* as it is coded by symbol **[0 1]**. This difference increases with SNR hence BER for MCD decreases with an increase in SNR.

F. Variation of residual ISI power with SNR

Ignoring the effect of noise to observe the ISI mitigation capability of CDD, we denote $N_{Y\text{total}}(i,t_2)$ as:

$$N_{Y\text{total}}(i,t_2) = N_Y(i,t_2) + ISI(i,t_2), \tag{34}$$

and $N_{Y\text{total}}(i,t_1)$ as follows:

$$N_{Y\text{total}}(i,t_1) = N_Y(i,t_1) + ISI(i,t_1). \tag{35}$$

In the above expressions, $N_Y(i,t_1)$ and $N_Y(i,t_2)$ denotes the desired signal in ith bit duration at times t_1 and t_2, respectively, $ISI(i,t_1)$, $ISI(i,t_2)$ be the inter-symbol-interference at times t_1 and t_2, respectively. Then if we subtract Eqn. (35) from Eqn. (34) we obtain the following:

$$N_Y(i,t_2) + ISI(i,t_2) - N_Y(i,t_1) - ISI(i,t_1), \tag{36}$$

or

$$N_Y(i,t_2) - N_Y(i,t_1) + ISI(i,t_2) - ISI(i,t_1). \tag{37}$$

From Fig. 4 it is evident that in case of *Bit-1* t_1 is very close to t_2 and the ISI signal decreases very gradually [49] as it has a long tail distribution. So, the following can be assumed:

$$ISI(i,t_1) \approx ISI(i,t_2). \tag{38}$$

Then Eqn. (38) reduces to the following expression:

$$N_Y(i,t_2) - N_Y(i,t_1), \tag{39}$$

which is the actual concentration difference at times t_1 and t_2, respectively. Hence ISI mitigation is achieved when a *Bit-1* is received.

In cases of *Bit-0* $N_Y(i,t_1)$ and $N_Y(i,t_2)$ are zero because no molecules are transmitted for sending *Bit-0*. So, Eqn. (37) reduces to the following expression:

$$ISI(i,t_2) - ISI(i,t_1). \tag{40}$$

It can be observed from Fig. 4 that ISI decreases with time. As an example, during 0.5s - 0.6s, $ISI(i,t_2) < ISI(i,t_1)$. So, (40) gives a negative concentration difference for *Bit-0*. CDD eliminates the ISI if *Bit-1* is received and utilizes the ISI signal to detect *Bit-0*. Thus, ISI is not detrimental in CDD. Further the residual ISI (plotted in Fig. 11) power is given by:

$$10\log_{10}\left[E(\sum_{i=1}^{L-1}(ISI(i,t_2) - ISI(i,t_1))^2/(L-1)\right]. \tag{41}$$

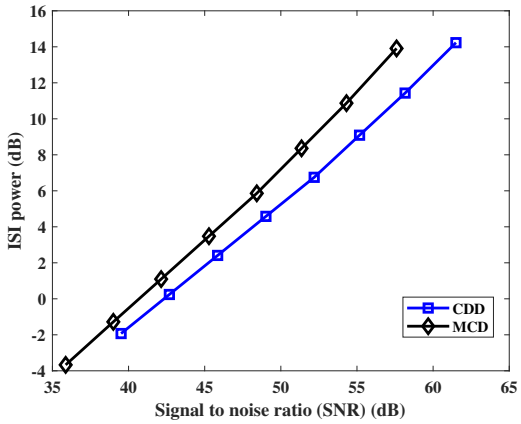

Fig. 11: Variation of residual ISI power with SNR with bit duration of 0.1s.

Having this residual ISI power, MCD can provide accurate detection. As evident in Fig. 5 that difference between consecutive peaks (Peak 1 - Peak 2) in a symbol is positive if *Bit-1* is received and the difference between consecutive peaks (Peak 5 - Peak 6) in a symbol is negative if *Bit-0* is received. So, accurate detection is possible. Also, ISI mitigation is achieved if such a concentration difference is taken as a decision metric as suggested in [49], where the effect of concentration difference for static MC is studied and no coding was used. So, if consecutive bits **[1 1]** or **[0 0]** are received their difference is zero. Hence, coding the *Bit-1* by symbol **[1 0]** and *Bit-0* by symbol **[0 1]** is necessary to differentiate between *Bit-1* and *Bit-0*. ISI power of the difference signal in MCD is calculated and plotted in Fig. 11 in a similar manner as CDD. The residual ISI power increases with an increase in SNR for the detectors CDD and MCD as shown in Fig. 11. As CDD utilizes the ISI to detect *Bit-0* hence some amount of ISI power is desirable in CDD. For MCD, the ISI is detrimental. Despite of ISI, MCD gives a better BER performance at 70 dB and 80 dB SNR values.

G. Comparative Perspectives

An overall comparison of different results are shown in Table I and Table IV. Table I presents some of the important results of the literature in this context and Table IV compares our detector performance with two other existing detectors. If the bit duration is 0.1s, SSD gives a data rate of 10bps but high BER. The BER decreases moderately with an increase in SNR. The BER decreases with an increase in bit duration because of reduced ISI. Also, for the same bit duration, SBD gives a data rate of 10bps and a relatively low BER than SSD. The BER decreases significantly with an increase in SNR. It is less robust to noise because the slope value is actually the difference between the concentration of consecutive samples, which can fluctuate rapidly with noise. CDD gives a data rate of 10bps and relatively low BER than SSD and SBD both. The BER decreases significantly with an increase in SNR. It is relatively more robust to noise because it calculates the largest concentration difference possible. CDD is less sensitive to ISI, as, it gives a low BER than SSD and SBD for less value of bit duration, 0.1s, which can be seen in Fig. 9(c). MCD gives a data rate of 5bps and a relatively lower BER than SSD, SBD and CDD. The BER decreases significantly with an increase in SNR. It is relatively more robust to noise than the other detectors because the concentration difference between peaks of consecutive bits in a symbol is taken which is expected to be positive for *Bit-1* and negative for *Bit-0*. Further MCD is less sensitive to ISI, as, it gives a low BER than SSD, SBD, and CDD for less value of bit duration, 0.1s, which can be seen in Fig. 9. Another advantage of CDD and MCD over other detectors is that both of these detectors do not need an adaptive threshold for detection in MMC.

TABLE IV: Comparison of Different Techniques

Parameters	**SSD** [33]	**SBD** [31]	**CDD**	**MCD**
SNR at BER 10^{-3}	-	75 dB	72 dB	69 dB
BER at SNR=70 dB with same bit duration=0.2	0.004	0.008	0.004	10^{-4}
BER at SNR=70 dB with same initial distance=10μm	0.1643	0.0051	0.002	0.0005
BER at SNR=70 dB with same bit sequence=6000	0.334	0.005	0.003	0.0006
Data rate (bps) at bit duration 0.1s	10	10	10	5

VII. Conclusion and Future Scopes

This work evaluated the performance of a new CDD technique for signal detection in an MMC scenario. A MCD technique has been also been explored. The differential detector calculates the difference between peaks of consecutive symbols. The detection threshold is selected using MAP rule, which is difficult in MMC. The proposed CDD and MCD techniques does not need an adaptive threshold to detect the bit. The performance of these detectors is compared with other existing detection techniques. Results reveal that CDD and MCD achieves a better BER performance than SSD and SBD even at 3 dB and 6 dB less SNR, respectively with other similar parameters. The proposed CDD and MCD techniques out perform other existing techniques in terms of different bit-sequence length, various initial distance and different bit

duration. Results show that the MCD technique is 3 dB less sensitive to ISI than CDD technique with a bit duration of 0.1s. With further reduction in bit duration, ISI causes errors in detection. If errors are more, nanomachines can not decode the commands correctly e.g., to increase or decrease the dosage of the drug. Future investigation includes detection techniques with ISI mitigation.

APPENDIX A
CALCULATION OF SIGNAL TO NOISE RATIO (SNR)

We show the calculation of SNR here. If we denote $\max(N_{Y\text{total}}(i,k))$ by X_i then Eqn. (25) can be written as

$$SNR = 10\log_{10}\left[\frac{E(\sum_{i=0}^{L-1} X_i^2)}{Lm_n}\right]. \tag{42}$$

Expanding the above equation results in

$$SNR = 10\log_{10}\left[\frac{E(X_0^2) + E(X_1^2) + ... + E(X_{L-1}^2)}{Lm_n}\right]. \tag{43}$$

Now, $E(X_i^2)$ can be found using the formula

$$variance = E(X_i^2) - (E(X_i))^2, \tag{44}$$

or

$$E(X_i^2) = variance + (E(X_i))^2. \tag{45}$$

Since, the received signal is poisson distributed, its mean and variance are equal. So,

$$E(X_i) = variance, \tag{46}$$

then,

$$E(X_i^2) = E(X_i) + (E(X_i))^2. \tag{47}$$

So, $E(X_i^2)$ can be found using above equation where $E(X_i)$ is expected maximum value of received signal in ith bit duration and can be calculated by finding the maximum value of Eqn. (19). L and m_n are total number bits transmitted and mean value of poisson distributed noise respectively. Both are constants, so SNR can be found using Eqn. (25).

REFERENCES

[1] T. Nakano, A. W. Eckford, and T. Haraguchi, *Molecular communication*. Cambridge University Press, 2013.

[2] F. Tavella, A. Giaretta, T. Dooley-Cullinane, M. Conti, L. Coffey, and S. Balasubramaniam, "DNA molecular storage system: Transferring digitally encoded information through bacterial nanonetworks," *IEEE Transactions on Emerging Topics in Computing*, vol. Early Access, pp. 1–1, 2019.

[3] U. Chude-Okonkwo, R. Malekian, and B. Maharaj, "Discussion on Advanced Targeted Nanomedical Application Scenarios for Treatment of Some Chronic Diseases," in *Advanced Targeted Nanomedicine*. Springer, Cham, 2019, ch. 7, pp. 125–143.

[4] M. H. Kassab, J. DeFranco, T. Malas, P. Laplante, g. destefanis, and V. V. Graciano Neto, "Exploring Research in Blockchain for Healthcare and a Roadmap for the Future," *IEEE Transactions on Emerging Topics in Computing*, pp. 1–1, 2019.

[5] S. Ghavami, F. Lahouti, and A. Masoudi-Nejad, "Modeling and analysis of abnormality detection in biomolecular nano-networks," *Nano Communication Networks*, vol. 3, no. 4, pp. 229–241, 2012.

[6] S. Ghavami and F. Lahouti, "Abnormality detection in correlated Gaussian molecular nano-networks: Design and analysis," *IEEE Transactions on Nanobioscience*, vol. 16, no. 3, pp. 189–202, 2017.

[7] A. Cavalcanti, T. Hogg, B. Shirinzadeh, and H. C. Liaw, "Nanorobot Communication Techniques: A Comprehensive Tutorial," in *2006 9th International Conference on Control, Automation, Robotics and Vision*, 2006, pp. 1–6.

[8] Q. Jiang, Z. Chen, J. Ma, X. Ma, J. Shen, and D. Wu, "Optimized Fuzzy Commitment based Key Agreement Protocol for Wireless Body Area Network," *IEEE Transactions on Emerging Topics in Computing*, pp. 1–1, 2019.

[9] A. A. Requicha, "Nanorobots, NEMS, and nanoassembly," *Proceedings of the IEEE*, vol. 91, no. 11, pp. 1922–1933, 2003.

[10] U. A. Chude-Okonkwo, R. Malekian, B. T. Maharaj, and A. V. Vasilakos, "Molecular communication and nanonetwork for targeted drug delivery: A survey," *IEEE Communications Surveys & Tutorials*, vol. 19, no. 4, pp. 3046–3096, 2017.

[11] T. Nakano, Y. Okaie, S. Kobayashi, T. Koujin, C. Chan, Y. Hsu, T. Obuchi, T. Hara, Y. Hiraoka, and T. Haraguchi, "Performance Evaluation of LeaderFollower-Based Mobile Molecular Communication Networks for Target Detection Applications," *IEEE Transactions on Communications*, vol. 65, no. 2, pp. 663–676, 2017.

[12] N. Varshney, W. Haselmayr, and W. Guo, "On flow-induced diffusive mobile molecular communication: First hitting time and performance analysis," *IEEE Transactions on Molecular, Biological and Multi-Scale Communications*, vol. 4, no. 4, pp. 195–207, 2018.

[13] R. Mosayebi, A. Ahmadzadeh, W. Wicke, V. Jamali, R. Schober, and M. Nasiri-Kenari, "Early cancer detection in blood vessels using mobile nanosensors," *IEEE Transactions on Nanobioscience*, vol. 18, no. 2, pp. 103–116, 2018.

[14] B. Tepekule, A. E. Pusane, H. B. Yilmaz, C.-B. Chae, and T. Tugcu, "ISI mitigation techniques in molecular communication," *IEEE Transactions on Molecular, Biological and Multi-Scale Communications*, vol. 1, no. 2, pp. 202–216, 2015.

[15] U. A. Chude-Okonkwo, R. Malekian, and B. S. Maharaj, "Molecular communication model for targeted drug delivery in multiple disease sites with diversely expressed enzymes," *IEEE Transactions on Nanobioscience*, vol. 15, no. 3, pp. 230–245, 2016.

[16] M. Femminella, G. Reali, and A. V. Vasilakos, "A molecular communications model for drug delivery," *IEEE Transactions on Nanobioscience*, vol. 14, no. 8, pp. 935–945, 2015.

[17] Y. Chahibi, M. Pierobon, S. O. Song, and I. F. Akyildiz, "A Molecular Communication System Model for Particulate Drug Delivery Systems," *IEEE Transactions on Biomedical Engineering*, vol. 60, no. 12, pp. 3468–3483, 2013.

[18] N. Farsad, H. B. Yilmaz, A. Eckford, C.-B. Chae, and W. Guo, "A comprehensive survey of recent advancements in molecular communication," *IEEE Communications Surveys & Tutorials*, vol. 18, no. 3, pp. 1887–1919, 2016.

[19] I. F. Akyildiz, F. Brunetti, and C. Blázquez, "Nanonetworks: A new communication paradigm," *Computer Networks*, vol. 52, no. 12, pp. 2260–2279, 2008.

[20] T. N. Cao, A. Ahmadzadeh, V. Jamali, W. Wicke, P. L. Yeoh, J. Evans, and R. Schober, "Diffusive Mobile MC With Absorbing Receivers: Stochastic Analysis and Applications," *IEEE Transactions on Molecular, Biological and Multi-Scale Communications*, vol. 5, no. 2, pp. 84–99, 2019.

[21] T. N. Cao, A. Ahmadzadeh, V. Jamali, W. Wicke, P. L. Yeoh, J. Evans, and R. Schober, "Diffusive mobile MC for controlled-release drug delivery with absorbing receiver," in *ICC 2019-2019 IEEE International Conference on Communications (ICC)*. IEEE, 2019, pp. 1–7.

[22] E. Gelenbe, "Errors and Power When Communicating With Spins," *IEEE Transactions on Emerging Topics in Computing*, vol. 3, no. 4, pp. 483–488, 2015.

[23] L. Felicetti, M. Femminella, G. Reali, and P. Liò, "A molecular communication system in blood vessels for tumor detection," in *Proceedings of ACM The First Annual International Conference on Nanoscale Computing and Communication*, 2014, pp. 1–9.

[24] S. Liu, P. Reviriego, and F. Lombardi, "Detection of Limited Magnitude Errors in Emerging Multilevel Cell Memories by One-Bit Parity (OBP) or Two-Bit Parity (TBP)," *IEEE Transactions on Emerging Topics in Computing*, pp. 1–1, 2019.

[25] A. Guney, B. Atakan, and O. B. Akan, "Mobile Ad Hoc Nanonetworks with Collision-Based Molecular Communication," *IEEE Transactions on Mobile Computing*, vol. 11, no. 3, pp. 353–366, 2012.

[26] I. F. Akyildiz, F. Brunetti, and C. Blázquez, "Nanonetworks: A new communication paradigm," *Computer Networks*, vol. 52, no. 12, pp. 2260–2279, 2008.

[27] L. Felicetti, M. Femminella, G. Reali, T. Nakano, and A. V. Vasilakos, "TCP-Like Molecular Communications," *IEEE Journal on Selected Areas in Communications*, vol. 32, no. 12, pp. 2354–2367, 2014.

[28] H. ShahMohammadian, G. G. Messier, and S. Magierowski, "Optimum receiver for molecule shift keying modulation in diffusion-based molecular communication channels," *Nano Communication Networks*, vol. 3, no. 3, pp. 183–195, 2012.

[29] A. Noel and A. W. Eckford, "Asynchronous peak detection for demodulation in molecular communication," in *2017 IEEE International Conference on Communications (ICC)*. IEEE, 2017, pp. 1–6.

[30] A. Noel, K. C. Cheung, and R. Schober, "Optimal receiver design for diffusive molecular communication with flow and additive noise," *IEEE Transactions on Nanobioscience*, vol. 13, no. 3, pp. 350–362, 2014.

[31] H. Yan, G. Chang, Z. Ma, and L. Lin, "Derivative-based signal detection for high data rate molecular communication system," *IEEE Communications Letters*, vol. 22, no. 9, pp. 1782–1785, 2018.

[32] B. Li, M. Sun, S. Wang, W. Guo, and C. Zhao, "Local convexity inspired low-complexity noncoherent signal detector for nanoscale molecular communications," *IEEE Transactions on Communications*, vol. 64, no. 5, pp. 2079–2091, 2016.

[33] A. Ahmadzadeh, V. Jamali, A. Noel, and R. Schober, "Diffusive mobile molecular communications over time-variant channels," *IEEE Communications Letters*, vol. 21, no. 6, pp. 1265–1268, 2017.

[34] N. Varshney, A. K. Jagannatham, and P. K. Varshney, "On diffusive molecular communication with mobile nanomachines," in *2018 52nd Annual Conference on Information Sciences and Systems (CISS)*. IEEE, 2018, pp. 1–6.

[35] G. Chang, L. Lin, and H. Yan, "Adaptive Detection and ISI Mitigation for Mobile Molecular Communication," *IEEE Transactions on Nanobioscience*, vol. 17, no. 1, pp. 21–35, 2018.

[36] S. Huang, L. Lin, W. Guo, H. Yan, J. Xu, and F. Liu, "Initial Distance Estimation and Signal Detection for Diffusive Mobile Molecular Communication," *IEEE Transactions on Nanobioscience*, pp. 1–1, 2020.

[37] X. Mu, H. Yan, B. Li, M. Liu, R. Zheng, Y. Li, and L. Lin, "Low-Complexity Adaptive Signal Detection for Mobile Molecular Communication," *IEEE Transactions on Nanobioscience*, vol. 19, no. 2, pp. 237–248, 2020.

[38] R. Mosayebi, V. Jamali, N. Ghoroghchian, R. Schober, M. Nasiri-Kenari, and M. Mehrabi, "Cooperative abnormality detection via diffusive molecular communications," *IEEE Transactions on Nanobioscience*, vol. 16, no. 8, pp. 828–842, 2017.

[39] R. Mosayebi, W. Wicke, V. Jamali, A. Ahmadzadeh, R. Schober, and M. Nasiri-Kenari, "Advanced target detection via molecular communication," in *2018 IEEE Global Communications Conference (GLOBECOM)*. IEEE, 2018, pp. 1–7.

[40] A. Cavalcanti, T. Hogg, B. Shirinzadeh, and H. C. Liaw, "Nanorobot communication techniques: A comprehensive tutorial," in *2006 9th International Conference on Control, Automation, Robotics and Vision*. IEEE, 2006, pp. 1–6.

[41] Y. Chahibi, M. Pierobon, S. O. Song, and I. F. Akyildiz, "A molecular communication system model for particulate drug delivery systems," *IEEE Transactions on Biomedical Engineering*, vol. 60, no. 12, pp. 3468–3483, 2013.

[42] N. Farsad and A. Goldsmith, "Neural network detection of data sequences in communication systems," *IEEE Transactions on Signal Processing*, vol. 66, no. 21, pp. 5663–5678, 2018.

[43] G. H. Alshammri, W. K. Ahmed, and V. B. Lawrence, "Receiver Techniques for Diffusion-Based Molecular Nano Communications Using an Adaptive Neuro-Fuzzy-Based Multivariate Polynomial Approximation," *IEEE Transactions on Molecular, Biological and Multi-Scale Communications*, vol. 4, no. 3, pp. 140–159, 2018.

[44] G. Chang, L. Lin, and H. Yan, "Adaptive detection and ISI mitigation for mobile molecular communication," *IEEE Transactions on Nanobioscience*, vol. 17, no. 1, pp. 21–35, 2017.

[45] M. Pierobon and I. F. Akyildiz, "Diffusion-based noise analysis for molecular communication in nanonetworks," *IEEE Transactions on Signal Processing*, vol. 59, no. 6, pp. 2532–2547, 2011.

[46] A. Ahmadzadeh, H. Arjmandi, A. Burkovski, and R. Schober, "Comprehensive reactive receiver modeling for diffusive molecular communication systems: Reversible binding, molecule degradation, and finite number of receptors," *IEEE Transactions on Nanobioscience*, vol. 15, no. 7, pp. 713–727, 2016.

[47] G. D. Ntouni, A. E. Paschos, V. M. Kapinas, G. K. Karagiannidis, and L. J. Hadjileontiadis, "Optimal detector design for molecular communication systems using an improved swarm intelligence algorithm," *Micro & Nano Letters*, vol. 13, no. 3, pp. 383–388, 2018.

[48] V. Jamali, A. Ahmadzadeh, and R. Schober, "Symbol synchronization for diffusion-based molecular communications," *IEEE Transactions on Nanobioscience*, vol. 16, no. 8, pp. 873–887, 2017.

[49] B. Li, M. Sun, S. Wang, W. Guo, and C. Zhao, "Low-complexity noncoherent signal detection for nanoscale molecular communications," *IEEE Transactions on Nanobioscience*, vol. 15, no. 1, pp. 3–10, 2015.

[50] Y. Hwang, J.-S. Kim, and I. S. Kweon, "Difference-based image noise modeling using skellam distribution," *IEEE Transactions on Pattern Analysis and Machine Intelligence*, vol. 34, no. 7, pp. 1329–1341, 2011.

Amit K. Shrivastava received the B.Tech. degree in Electronics and Communication engineering from the National Institute of Technology, Raipur in 2010, the M.Tech. degree in Digital Communication from Atal Bihari Vajpayee-Indian Institute of Information Technology and Management, Gwalior, in 2013, and is currently pursuing Ph.D. degree in Electronics and Communication engineering from Dr. SPM IIIT Naya Raipur.

Debanjan Das (M'11) received the B.Tech. degree in applied Electronics and Instrumentation engineering from the Heritage Institute of Technology, Kolkata, in 2009, the M.Tech. degree in Instrumentation from Indian Institute of Technology, Kharagpur, in 2011, and the Ph.D. degree in Electrical Engineering from Indian Institute of Technology, Kharagpur, in 2016. He is an Assistant Professor with Dr. SPM IIIT Naya Raipur.

Rajarshi Mahapatra received the Ph.D. degree in Electronics and Electrical Communication engineering from the Indian Institute of Technology Kharagpur, Kharagpur, India, and the postdoctoral degree from the Commissariat lnergie Atomique et aux nergies, Grenoble, France He is Associate Professor with the Department of Electronics and Communication Engineering, Dr. SPM IIIT Naya Raipur. He is also handling the responsibilities of Dean (Academics) of IIITNR.

Saraju P. Mohanty (SM'08) received the bachelor's degree (Honors) in electrical engineering from the Orissa University of Agriculture and Technology, Bhubaneswar, in 1995, the masters degree in Systems Science and Automation from the Indian Institute of Science, Bengaluru, in 1999, and the Ph.D. degree in Computer Science and Engineering from the University of South Florida, Tampa, in 2003. He is a Professor with the University of North Texas. His research is in "Smart Electronic Systems" which has been funded by National Science Foundations (NSF), Semiconductor Research Corporation (SRC), U.S. Air Force, IUSSTF, and Mission Innovation. He has authored 350 research articles, 4 books, and invented 4 U.S. patents. His Google Scholar h-index is 36 and i10-index is 134 with 5900 citations.